STUDY OF TURBULENT BOUNDARY LAYERS ON SMOOTH AND ROUGH SURFACES WITH ARBITRARY PRESSURE GRADIENTS

A. G. Marchenko

The results of an experimental investigation into the steady-state plane turbulent boundary layer in an incompressible liquid at an impermeable wall are presented. Cases of flow at smooth and rough surfaces in the presence of a longitudinal pressure gradient are considered. The results of measurements of the turbulent structure of the flow at various distances from the channel inlet are presented. A detailed analysis of the kinematic and dynamic characteristics of the flow is given. Special attention is paid to the boundary region of the flow close to the wall. A universal law is proposed for the variation in the local resistance coefficient along the boundary layer.

Notation: U, V, longitudinal and transverse components of the average velocity; u, v, components of the velocity pulsations; P, average pressure; τ, tangential stress; u_*, dynamic velocity; C_f, local coefficient of surface friction; ρ, density; ν, kinematic molecular viscosity; ε, effective viscosity; δ, thickness of the sublayer close to the wall; s, thickness representing the range of action of the wall law; h, thickness of the boundary layer; x,y, space coordinates; T, time of averaging the velocity in photographic recording.

The indices denote: 0, at the wall; δ, at the outer edge of the wall sublayer; s, at the boundary of the range of action of the wall law; ∞, at the outer edge of the boundary layer.

1. Experimental Arrangement. The experiments were carried out in a hydrodynamic test-bed of periodic action with a vertically placed working section (Fig. 1). This was connected to a pressure tank in order to ensure smooth entry. In order to eliminate vibration when the jet entered the receiving tank, dampers were provided. At the exit from the working channel a regulating device was installed to maintain a steady flow of water. Using a system of pulleys, the axle of the regulator shutter was connected to a float in the pressure tank, and the specified mode of flow was thus automatically controlled. The water was returned from the receiver to the pressure tank by means of a pump. Filling continued up to a specified working mark. On rising to the specified position, the float closed a relay contact, interrupted the electrical supply circuit, and automatically disconnected the pump. After the water had settled in the pressure tank for 5 min, the system was started and the working cycle executed.

The working part had a rectangular section of $a \times b = 10 \times 30$ cm^2 and glass walls. Inside this part of the system were two interchangeable, symmetrically placed, movable plates ($b \times l = 30 \times 70$ cm^2) enabling the cross section of the test part to be varied.

Smooth plates were made of 7-mm glass. In order to eliminate the laminar part of the boundary layer, a rough surface d = 1.5 mm in height was placed on the first 3 cm of the plates starting from the leading edge. The rough plates were prepared by sticking gravel grains on the glass surface with epoxy resin (layer $t \approx 0.5$ mm). Fractions of gravel with a particle diameter of 1 and 2 mm were taken in equal proportions and carefully mixed. After application of the rough surface, a thin layer of nitro lacquer was deposited by means of a pulverizer.

Kiev. Translated from Zhurnal Prikladnoi Mekhaniki i Tekhnicheskoi Fiziki, No. 3, pp. 126-134, May-June, 1971. Original article submitted October 26, 1970.

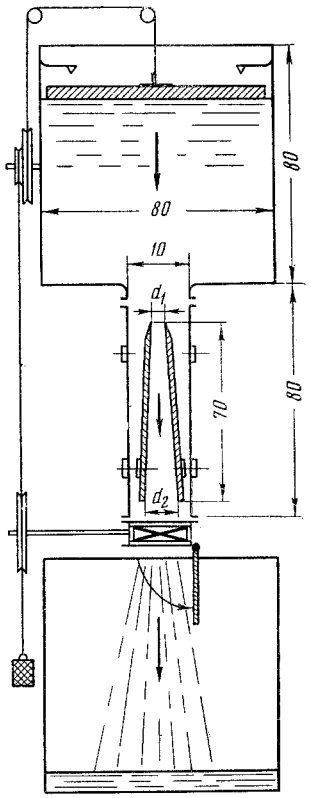

Fig. 1. Arrangement of experimental apparatus (version with expanding channel).

The structure was measured by microphotography of the flow, the latter being illuminated in individual flashes through a narrow slot; the experimental data were analyzed statistically. A detailed description of the method of investigation and of the electronic flash equipment was given in [1, 2].

Let us briefly mention the method of determining certain characteristics of the flow which will be used subsequently in analyzing the experimental data.

The thickness of the boundary layer h was determined in the present investigation by reference to the points at which the distributions of the average and pulsating velocities passed into the form of a straight line, corresponding to the values of these characteristics in the potential core of the flow, and also by reference to the point on the distribution of correlation moments at which $\langle uv \rangle$ vanished.

The thickness of the inner region of the boundary layer s was determined by reference to the point on the distribution of $U = f(y)$ at which a deviation from the logarithmic profile calculated by means of Eq. (2.1) (see below) began to appear.

From the change in the velocity of the external flow we found the pressure gradients by using the relation [3]

$$U_\infty \frac{dU_\infty}{dx} = -\frac{1}{\rho}\frac{dP_\infty}{dx} \qquad (1.1)$$

The velocity gradients dU/dy were determined graphically and analytically. The results of the two methods agreed closely with one another.

2. Results of the Experiment. We studied three characteristic cases of a turbulent boundary layer developing on smooth and rough surfaces in a channel with parallel, contracting, or expanding walls. We made seven series of experiments and measured the structure of the flow in cross sections lying at different distances from the inlet. The seventh series constituted a repetition of the sixth on a larger scale in the region of flow close to the wall. The fact that the original and repeated results agreed with one another proved the reproducibility and reliability of the experimental results.

In addition to this we measured the structure of the flow directly in front of the leading edge of the plates forming the working channel so as to be able to judge the characteristics of the incident flow. We found that the distribution of averaged longitudinal velocities had a rectangular form. We noted the existence of a transverse velocity which might give rise to a slight eddy at the leading edge of the plate, drawing the flow in at the entrance into the channel. The correlation moments $\langle uv \rangle = 0$. The relative intensity of the turbulence of the incident flow

$$\frac{\sqrt{\langle u \rangle^2 + \langle v \rangle^2}}{U_\infty} \approx 5\%$$

Our investigations covered the range of Reynolds numbers $R_x = 5 \cdot 10^3$–$5 \cdot 10^5$. The original data are presented in Table 1.

Here the ratios $d_1/d_2 = 1.0$, 2.2, and 0.455 characterize channels with parallel ($d_1 = d_2 = 4.0$ cm), contracting ($d_1 = 6.6$ cm, $d_2 = 3.0$ cm), and expanding ($d_1 = 3.0$, $d_2 = 6.6$ cm) walls; the asterisks on the numbers of some series indicate a rough surface; the time of averaging the velocity in the photorecording T = 0.00092 sec for series 1, 2, 3, 4, 5, 6 and T = 0.000035 sec for the seventh series; the kinematic molecular viscosity $\nu = 0.0100$, 0.0115, 0.01035 for series 1, 2, 4, and $\nu = 0.0117$ for 3, 5, 6, 7.

The results of the present investigation were principally compared with the experimental data relating to flow in a turbulent boundary layer at a smooth wall obtained by Kline, Reynolds, Schraub, and Runstabler [4] for various pressure gradients.

TABLE 1.

$\frac{d_1}{d_2}$	Series No.	Expt. No.	x, cm	h, cm	U_∞, cm/sec	$\frac{P'_\infty}{\rho}$	$R_x = \frac{U_\infty x}{\varepsilon_\delta}$
		1	7	0.50	69.0	—0.0162	$4.39 \cdot 10^4$
		2	20	0.75	74.0	—0.0173	$1.48 \cdot 10^5$
	1	3	31	1.05	72.0	—0.0169	$2.23 \cdot 10^5$
		4	44	1.25	74,0	—0.0173	$3.25 \cdot 10^5$
1.0		5	59	1.60	82.0	—0.0193	$4.84 \cdot 10^5$
		6	5	0.60	70.6	—0.0165	$5.05 \cdot 10^3$
		7	15	1.00	75.5	—0.0177	$1.67 \cdot 10^4$
	2*	8	26	1.30	79.0	—0.0186	$3.08 \cdot 10^4$
		9	40	1.60	82.0	—0.0193	$4.55 \cdot 10^4$
		10	59	1.80	84.0	—0.0197	$6.70 \cdot 10^4$
		11	6	0.35	55.3	—0.0161	$2.84 \cdot 10^4$
		12	15	0.55	56.5	—0.0164	$7.25 \cdot 10^4$
	3	13	30	0.80	61.0	—0.0177	$1.56 \cdot 10^5$
		14	55	0.95	69.5	—0.0202	$3.25 \cdot 10^5$
2.2		15	5	0.45	57.3	—0.0239	$4.95 \cdot 10^3$
	4*	16	22	0.95	64.5	—0.0269	$3.02 \cdot 10^4$
		17	38	1.10	70.3	—0.0298	$4.86 \cdot 10^4$
		18	59	1.25	80.0	—0.0334	$8.31 \cdot 10^4$
		19	8	0.80	110.0	+0.0443	$7.51 \cdot 10^4$
	5	20	18	1.40	105.5	+0.0425	$1.65 \cdot 10^5$
		21	35	1.90	98.5	+0.0396	$2.95 \cdot 10^5$
		22	58	2.10	90.5	+0.0364	$4.50 \cdot 10^5$
		23	6	0.75	111.0	+0.0192	$8.42 \cdot 10^3$
0.455	6*	24	18	1.55	109.0	+0.0189	$2.95 \cdot 10^4$
		25	35	2.15	107.5	+0.0186	$5.79 \cdot 10^4$
		26	55	2.40	103.0	+0.0179	$9.76 \cdot 10^4$
		27	6	0.75	—	+0.0192	$8.42 \cdot 10^3$
	7*	28	18	1.55	—	+0.0189	$2.95 \cdot 10^4$
		29	35	2.15	—	+0.0186	$5.79 \cdot 10^4$
		30	55	2.40	—	+0.0179	$9.76 \cdot 10^4$

Averaged Velocities. The distribution of the averaged flow velocities is shown in dimensionless form $U/U_\delta = f(\log y/\delta)$ in Fig. 2. In order to describe the velocity profile in the range of action of the wall law ($\delta \leq y \leq s$) and in the wall sublayer δ we used relationships based on the two-layer model of flow [5]. These we may write in the following manner:

$$1 \leqslant \frac{y}{\delta} \leqslant \frac{s}{\delta}, \quad \frac{U}{u_{*\delta} R_{*\delta}} = 1.15 \lg \frac{y}{\delta} + 1.5 - 0.5 \frac{\delta}{y} \tag{2.1}$$

$$0 \leqslant \frac{y}{\delta} \leqslant 1, \quad \frac{U}{u_{*\delta} R_{*\delta}} = \frac{y}{\delta} \qquad \left(R_{*\delta} = \frac{u_{*\delta}}{\varepsilon_\delta}\right) \tag{2.2}$$

The product $u_{*\delta}\, R_{*\delta}$ by which the averaged flow velocities are normalized is a real physical quantity – the rate of flow at the boundary of the sublayer. It follows from (2.1) and (2.2), in fact, that at $y = \delta$

$$U_\delta \equiv u_{*\delta} R_{*\delta} \tag{2.3}$$

Thus, the relationship used for describing the velocity profile in the region next to the wall contains two unknown quantities δ and U_δ. For the determination of these we used Eq. (2.1) and the measured $U = f(y)$ profile. Substituting the values of y_i and U_i at two arbitrarily chosen points on the velocity distribution belonging to the logarithmic region ($\delta < y < s$) into (2.1), we solve the system of two equations with two unknowns and find the values of δ and U_δ.

The dynamic velocity, or the velocity of friction, is by definition expressed thus:

$$u_* \equiv \sqrt{\tau_0/\rho}$$

By analogy with this,

$$u_{*\delta} \equiv \sqrt{\tau_\delta/\rho} \quad \text{at} \quad y = \delta \tag{2.4}$$

The values of the parameter $R_{*\delta}$ characterizing the energy processes taking place in the flow layers close to the wall [5] may be found as a fraction by dividing (2.3) by (2.4).

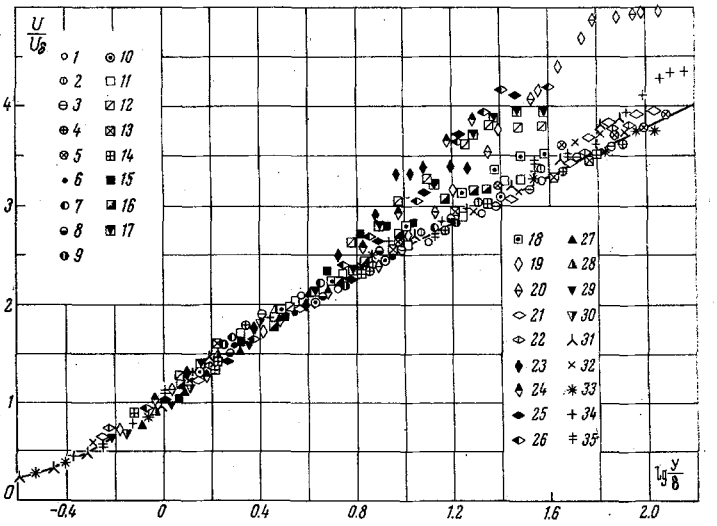

Fig. 2. Dimensionless velocity profile in a turbulent boundary layer. Author's measurements at a smooth and rough wall: 1-5) series 1; 6-10) series 2, $P' < 0$; 11-14) series 3; 15-18) series 4, $P' < 0$; 19-22) series 5; 23-26) series 6; 27-30) series 7, $P' > 0$; the enumeration of the points corresponds to the enumeration of the experiments in Table 1. Measurements of Kline et al. [4] on a smooth surface: 31) $P' = 0$; 32) $P' < 0$; 33) $P' \ll 0$; 34) $P' > 0$; 35) $P' \gg 0$.

The effective viscosity is a simple combination

$$\varepsilon \equiv \nu_T + \nu \tag{2.5}$$

The turbulent viscosity (Bussinescu) is given by the expression

$$-\langle uv\rangle \equiv \nu_T dU/dy$$

We may therefore write

$$\tau/\rho \equiv -\langle uv\rangle + \nu dU/dy = \varepsilon dU/dy$$

It follows from this that

$$\varepsilon = \frac{\tau/\rho}{dU/dy} \quad \text{or} \quad \varepsilon = \nu - \frac{\langle uv\rangle}{dU/dy} \tag{2.6}$$

At the boundary of the wall sublayer δ we then find, after appropriate transformations of (2.6),

$$\varepsilon_\delta = \frac{u_{*\delta}\delta}{R_{*\delta}}$$

which also follows directly from (2.2).

We note that in the case of flow at a smooth surface $\varepsilon_\delta = \nu$.

The experimental data indicate the existence of a local similarity of the flow close to the wall in the boundary layer with nonzero pressure gradients and confirm the universality of the wall law. This important result has been generally accepted and forms the basis of a number of present-day methods of calculating the turbulent boundary layer.

The distribution of averaged velocities on smooth and rough surfaces is represented by a single universal relationship. It is usually considered that in the logarithmic region the influence of roughness manifests itself solely as a displacement of the velocity profile in the semilogarithmic axes. However, owing to the variety of geometrical shapes characterizing the elements of roughness, a large number of parameters is required in order to describe the properties of the surface, and this makes the problem far more

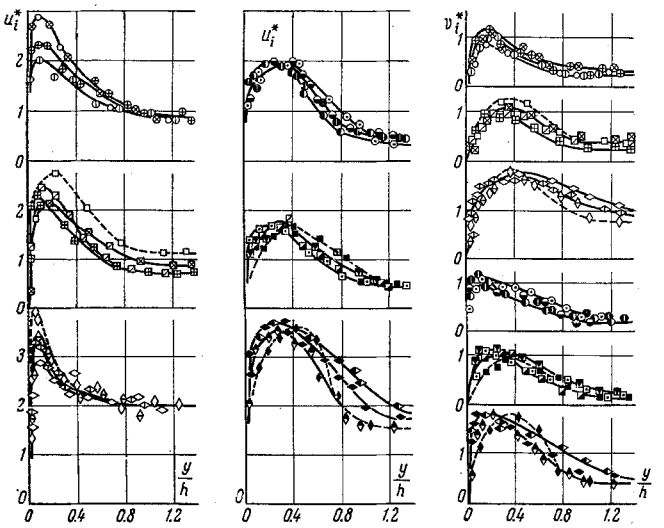

Fig. 3. Intensity profiles of the longitudinal and transverse velocity pulsations u_i^* and v_i^* at various distances from the channel inlet; the broken profile relates to the first cross section. The notation of the points is the same as in Fig. 2.

complicated. On using Eq. (2.1), the influence of the rough properties of the surface is completely taken into account by the thickness of the wall sublayer δ and the effective viscosity ε_δ at its outer boundary, and this leads to a universal form of the velocity profile. This simplifies the problem and offers analytical convenience, thus providing a good basis for developing new methods of theoretically calculating the turbulent boundary layer.

The logarithmic velocity profile may, to a fair degree of accuracy, be extended to the whole thickness of the boundary layer for a certain class of flows. This holds true for the majority of flows in tubes and channels, for many cases of a turbulent boundary layer on a plate, and in the initial parts of channels with zero and negative pressure gradients. Many investigations by a wide variety of authors (and to some extent the data of Fig. 2) act as a basis for this.

The outer region of the boundary layer will not be considered in detail in this paper. We shall simply observe that experimental data indicate the absence of similarity in the profiles of the velocity defect (deficiency) in the case of flow through contracting and expanding channels, i.e., in these cases a nonequilibrium turbulent boundary layer develops.

3. Pulsations and Friction. Velocity pulsations. For negative pressure gradients (channels with parallel and contracting walls) the absolute values of the velocity pulsation components $\sqrt{\langle u^2\rangle}$ and $\sqrt{\langle v^2\rangle}$ increase monotonically in the direction of the flow, while for positive pressure gradients (expanding channel) they diminish. In all cases studied the distributions of the longitudinal pulsations have a sharply expressed maximum close to the smooth wall, lying slightly above the boundary of the wall sublayer; for flow on a rough surface the maximum of $\sqrt{\langle u^2\rangle}$ moves into the core of the boundary layer. The distributions of the transverse velocity pulsations vary smoothly in all cases; their maximum value occurs within the thickness of the boundary layer. The ordinate of the maximum is not constant.

The intensity distribution of the velocity pulsations in cross sections of the boundary layer lying at various distances from the channel entrance is illustrated in Fig. 3. Exactly the same qualitative picture appears here; at the smooth surfaces the intensity of the longitudinal pulsations

$$u_i^* = \left(\sqrt{\langle u^2\rangle}/u_*\right)_{\max} \tag{3.1}$$

is greater and that of the transverse pulsations

$$v_i^* = \left(\sqrt{\langle v^2\rangle}/u_*\right)_{\max} \tag{3.2}$$

is smaller than at the rough surfaces.

The intensity of the turbulence is greatly increased by positive external pressure gradients. The mean square values of the velocity pulsations at the outer edge of the boundary layer depend on the degree of turbulence of the potential core of the flow.

The measured intensities of the velocity pulsations associated with flow on a smooth wall with negative pressure gradients were compared with the experimental results of Laufer [6], Cont-Bello [7], and Clark [8]. Excellent basic agreement was obtained between these data. We should mention one particular point, however. Cont-Bello indicates that the intensities of the pulsations increase monotonically in the direction of flow. According to the results obtained here, these values fall in the first three sections, but in the fourth section the sign representing the evolution of this distribution changes. An exactly analogous picture is obtained for flow at a smooth wall with a positive pressure gradient. At any rate, this certainly applies to the maximum values of the longitudinal velocity pulsations. A number of factors arising from peculiarities concerning the entry of the flow into the channel may be used to explain these differences.

Turbulent friction. Figure 4a, b illustrates the distribution of turbulent friction normalized with respect to the square of the dynamic velocity. For flow on both smooth and rough surfaces (other conditions being equal) the distribution

$$\tau = \langle uv \rangle / u_*^2 = f(y/h) \tag{3.3}$$

may be approximated by a single relationship to an accuracy equivalent to the experimental error.

Positive pressure gradients produce a very substantial increase in turbulent friction and displace its maximum into the core of the boundary layer.

Figure 4a, b illustrates the distribution of turbulent friction $\langle uv \rangle$, using a transverse displacement correlation coefficient

$$\varkappa = \frac{\langle uv \rangle}{\langle u^2 \rangle \langle v^2 \rangle} \tag{3.4}$$

The value is zero at the wall and tends toward zero at the outer edge of the boundary layer; in the region between the immediate vicinity of the wall and $y/h \approx 0.7$ the correlation coefficient is almost constant. The scatter in the experimental points does not exhibit any particular tendency, and may thus be ascribed to experimental error. To a fair degree of reliability we may consider that the distribution of the correlation coefficient does not depend very greatly on the longitudinal coordinate x, the roughness of the walls, or the pressure gradient.

Comparison with the measurements of Klebanoff [9] (on a flat plate), Laufer [6] (in a smooth round tube), and Cont-Bello [7] (in a plane parallel channel with smooth walls) indicates that the manner in which the correlation coefficient is distributed over the cross section of the flow is exactly the same for all cases of flow considered. However, the maximum values of the correlation coefficient differ for different forms of flow, being equal to 0.5 for a boundary layer on a flat plate, 0.45 for flow in a round tube, and 0.39-0.41 for flows in the initial sections of plane channels with smooth and rough walls for various pressure gradients.

Tangential stresses at the wall. The measurements of the turbulent structure carried out in the present investigation partly included the region of the sublayer close to the wall. Thus we may use our experimental data to determine the total tangential stress at a very short distance from the wall $y = \delta$. Then

$$\tau_\delta = \rho (\langle -uv \rangle + \nu dU/dy)_\delta \tag{3.5}$$

The tangential stress at the wall may be determined if we allow for the effect of the pressure gradient by means of the additional term $y dP_\infty/dx$ [3]. Then, for $y = 0$,

$$\tau_0 = \tau_\delta - \delta \, dP_\infty / dx \tag{3.6}$$

Coefficient of surface friction. The local surface-friction coefficient defined by the expression

$$C_f = 2\tau_0 / \rho U_\infty^2 \tag{3.7}$$

depends on the Reynolds number, the surface roughness, and the magnitude and sign of the pressure gradient. A number of relationships have been proposed for determining C_f, each giving satisfactory results for a comparatively narrow range of conditions. Attempts at establishing universal relationships for calcu-

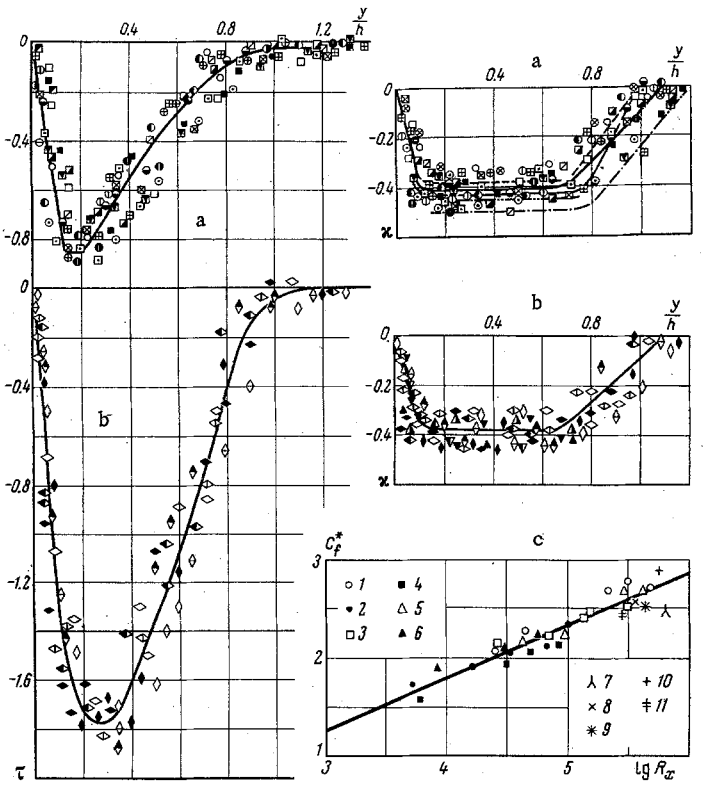

Fig. 4. Distribution of the stress due to turbulent friction τ and the correlation coefficients $\varkappa$ in the boundary layer at smooth and rough surfaces for negative (a) and positive (b) pressure gradients. In the case of the points the notation of Fig. 2 has been retained; the broken lines with two dots represent stabilized flow according to the measurements of Laufer [6], the ordinary broken lines, Cont-Bello [7], the broken lines with one dot, Klebanov [9]. The universal form of the relationship between the local surface-friction coefficient and the R_x number is given in (c). The author's experimental data for the smooth and rough surfaces, respectively, are represented thus: 1,2) P' = 0 (plane-parallel channel); 3,4) P' < 0 (contracting channel); 5,6) P' > 0 (expanding channel). The numbers of the points correspond to the numbers of the series. Kline et al.'s data [4] for the smooth surface are given by: 7) P' = 0; 8) P' < 0; 9) P' $\ll$ 0; 10) P' > 0; 11) P' $\gg$ 0.

lating the distribution of tangential stresses and the coefficients of surface friction have not yet been successful. A detailed analysis of the present state of the problem was presented in [3]. Experiment should play the major part in solving this problem.

By analyzing the data already obtained, we were able to find some dimensionless relationships for the flow parameters, leading to a universal empirical relationship of the form

$$\frac{1}{\sqrt{C_f}} = R_{*\delta}\left(\frac{U_\infty}{U_s}\right)^{1/2}(0.52\lg R_x - 0.32) \qquad (3.8)$$

The results of calculations relating to the whole range of conditions studied are presented in Fig. 4c in coordinates of

$$\ln R_x, \quad C_f^* = \frac{1}{\sqrt{C_f}\,R_{*\delta}\sqrt{U_\infty/U_s}}$$

The scatter in the experimental points is no greater than 10%.

The experimental data regarding the turbulent boundary layer at a smooth wall obtained for five pressure gradients of different magnitudes and signs by Kline, Reynolds, Schraub, and Runstadler [4] agree quite satisfactorily with (3.8) and thus enable us to extend the use of this equation to a wider range of conditions.

The use of Eq. (3.8) for calculating the coefficient of friction C_f is in practice permissible if we know the velocity distribution $U = f(y)$ in the cross sections of the boundary layer, at any rate for flow on smooth surfaces; in the case of rough surfaces we must also possess additional information regarding the Reynolds stresses $\langle uv \rangle$ close to the wall. We may then determine the initially unknown values of $R_{*\delta}$ and U_∞/U_S by the method just proposed.

For cases of zero pressure gradients, when the logarithmic profile of the velocities may be extended to the whole thickness of the boundary layer, the problem simplifies

$$U_\infty / U_s = 1$$

and the value of $R_{*\delta}$ is found [10] from the equation

$$R_{*\delta} = \frac{R_{*\delta\infty}}{\psi(h/\delta)}, \quad \psi\left(\frac{h}{\delta}\right) = \left(\frac{h/\delta - 1}{h/\delta}\right)^{1/2}\left(1 - \frac{\delta}{h}\right) \tag{3.9}$$

The quantity $R_{*\delta\infty}$ has a constant value for a particular type of roughness. This question was discussed in detail in [10].

LITERATURE CITED

1. V. S. Nishchuk and A. G. Marchenko, "Study of macroturbulence by microphotography of the flow," in: Hydraulics and Hydrotechnology, No. 7 [in Russian], Tekhnika, Kiev (1968).
2. E. M. Egidis, V. S. Nishchuk, A. G. Marchenko, and V. I. Ratskii, "Flash lighting system for studying the high-speed structure of flows," in: Hydraulics and Hydrotechnology, No. 8 [in Russian], Tekhnika, Kiev (1969).
3. I. K. Rotta, Turbulent Boundary Layer in an Incompressible Liquid [in Russian], Sudostroenie, Leningrad (1967).
4. S. J. Kline, W. C. Reynolds, F. A. Schraub, and P. W. Runstabler, "The structure of turbulent boundary layers," J. Fluid Mech., 30, Pt. 4 (1967).
5. I. K. Nikitin, "Generalized relationships for calculating stabilized turbulent flows based on a two-layer principle," in: Homogeneous and Suspension-Carrying Turbulent Flow [in Russian], Naukova Dumka, Kiev (1967).
6. J. Laufer, "The structure of turbulence in fully-developed pipe flow," NACA, Rept. No. 1175 (1954).
7. G. Cont-Bello, Turbulent Flow in a Channel with Parallel Walls [Russian translation], Mir, Moscow (1968).
8. Clark, "Study of an incompressible turbulent boundary layer during flow in a channel," Transactions of the ASME, Theoretical Fundaments of Engineering Calculations, No. 4 [Russian translation] (1968).
9. P. S. Klebanoff, "Characteristics of turbulence in a boundary layer with zero pressure gradient," NACA, Rept. No. 1247 (1955).
10. I. K. Nikitin, "Two-layer scheme for calculating a turbulent boundary layer at a plate with arbitrary roughness," in: Study of Turbulent One- and Two-Phase Flows [in Russian], Naukova Dumka, Kiev (1966).